Scattering from an elastic cylinder buried beneath a rough water/sediment interface

John A. Fawcett

SACLANT Undersea Research Centre
Viale San Bartolomeo, 400
19138 La Spezia, ITALY
E-mail: fawcett@saclantc.nato.int

Abstract

In this paper a plane-wave decomposition method is used to compute the two-dimensional backscattering from a buried elastic cylinder as a function of frequency. The cases of a flat water/sediment interface and deterministically rough interfaces are considered. For rough interfaces, first-order perturbation theory is utilized to compute the interface reflection and transmission scattering matrices. In particular, the situation where the grazing angle in the water column is sub-critical is considered. In this case, at sufficiently high frequencies, the energy scattered into the bottom by the rough interface is dominant. The amplitude and spectral characteristics of the energy backscattered by the interface itself are also computed. Finally, the accuracy of using a simpler, single-scatter approximation is examined.

1. INTRODUCTION

In this paper, the backscattering from an elastic-shelled cylinder buried in sediment is considered. In particular, the grazing angle of the incident beam is taken to be subcritical. In this case, most of the energy transmitted into the bottom is evanescent and for sufficiently high frequencies it would be expected that very little of this energy would interact with the buried cylinder. However, some experiments [1],[2] have indicated that an anomalously large amount of energy does, in fact, penetrate into the bottom. Two possible explanations for this high level of energy are: (1) the existence of a Biot slow wave in the bottom [2,3], (2) a rough water/sediment interface which causes energy to be scattered into the bottom [4]. In this paper, the latter concept is investigated numerically. However, instead of simply considering the amount of energy which propagates in the bottom, the amplitude of the field backscattered from a buried steel-shelled cylinder is examined. The amplitude of this backscattered signal relative to the noise generated by the rough interface itself is also considered.

The plane-wave decomposition method for object and bathymetric scattering (see, for example [5],[6]) is used as the computational tool. We investigate burial below both flat and rough interfaces. For the case of a rough interface, first-order perturbation theory is used to compute the plane-wave scattering matrices for the interface. First-order perturbation theory has been shown by other authors [7] to be surprisingly accurate for the computation of the transmitted field. There has also been related work [8] for the case of an elastic sphere buried below a rough elastic interface.

2. THEORY

We consider a plane-wave incident upon an infinite elastic cylinder with an angle of incidence of θ_{in}. The cylinder is taken to be surrounded by a fluid with sound speed c_{se} and density ρ_{se}. The compressional potential scattered by the cylinder has the form

$$\phi_p^{sc} = \sum_{n=-\infty}^{\infty} \alpha_n H_n^1(k_{se} r) e^{in(\theta - \theta_{in})} \tag{1}$$

where α_n are coefficients determined from the solution of a system of equations. This system of equations is derived by assuming Fourier-Bessel series for compressional and shear potentials within the layers of the cylinder and then satisfying the appropriate continuity conditions across interfaces.

The individual azimuthal terms of (1) have a plane-wave decomposition given by:

$$H_n^1(kr)e^{in\theta} = \frac{e^{-in\pi/2}}{\pi} \int_C \frac{e^{i(k_x x + \gamma_{se}(k_x)z)} e^{in\beta(k_x)}}{\gamma_{se}(k_x)} dk_x \tag{2}$$

where "C" is an appropriate contour in the complex-k_x plane, $\beta(k_x)$ is the angle associated with the horizontal wavenumber k_x, and γ_a is defined in general as

$$\gamma_a = \sqrt{\frac{\omega^2}{c_a^2} - k_x^2}. \tag{3}$$

Using (2) with (1) it is thus possible to express the scattered field in terms of plane-waves. We will discretize the integral of (2). In this case, the effect of the cylinder on incident plane-waves is characterized by a finite matrix.

For a buried cylinder, the water/sediment interface modifies the incident field and also rescatters the scattered field from the cylinder. By characterizing the interface and cylinder in terms of plane-wave scattering matrices (or for a continuous spectrum, operators) we can express the vector of plane-wave components, $\vec{P}^u$ for the scattered field in the water column as,

$$\vec{P}^u = T_{UU}[I - \tilde{C}\tilde{R}_{UD}]^{-1}\tilde{C}\Phi_D T_{DD}\vec{P}^{in} \tag{4}$$

where $\vec{P}^{in}$ is the vector of incident plane-wave components. In (4) T_{UU} and T_{DD} denote transmission matrices for downgoing and upgoing plane-waves across the interface. For a flat interface, these matrices are diagonal. For a non-flat interface, a single plane-wave will scatter into a continuum of other plane-waves and these matrices will be full. The matrix Φ_D is diagonal and advances the vertical phases of the downgoing waves between the interface and the cylinder centre. For propagating waves these phase factors have unity norm; for evanescent waves these factors are decaying exponentials. Finally, $\tilde{C} \equiv \Phi_U C$ and $\tilde{R}_{UD} \equiv \Phi_D R_{UD}$ where C is the scattering matrix for the cylinder (for the scattering of downward incident plane-waves into upgoing plane-waves) ,R_{UD} is the interface reflection matrix for upgoing waves in the basement and Φ_U advances the phases of upgoing plane-waves. A schematic diagram of the scattering geometry with some of the operators indicated is shown in Fig. 1

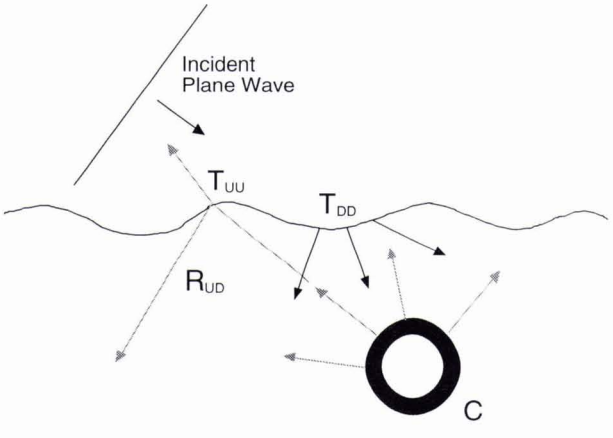

Figure 1: *A schematic of the scattering geometry*

In the case of a non-flat interface, it is non-trivial to compute the elements of T_{DD},T_{UU} and R_{UD} for general interfaces. We will assume that the interface is of the form

$$z = z_0 + h(x) \tag{5}$$

where $h(x)$ is much smaller in amplitude than a wavelength and that first-order perturbation theory will suffice to compute the scattering coefficients. In order to derive the perturbation theory the compressional potential in

the water, ϕ_w is taken to have the form

$$\phi_w = e^{i(k_0 x - \gamma_0 z)} + R_0 e^{i(k_0 x + \gamma_w z)} + \int_{-\infty}^{\infty} a(\lambda) e^{i(\lambda x + \gamma_w(\lambda) z)} d\lambda \tag{6}$$

and in the sediment the compressional potential ϕ_{se} has the form

$$\phi_{se} = T_0 e^{i(k_0 x + \gamma_{se} z)} + \int_{-\infty}^{\infty} b(\lambda) e^{i(\lambda x - \gamma_{se}(\lambda) z)} d\lambda, \tag{7}$$

where γ_w and γ_{se} are the vertical wavenumbers in the water and sediment respectively. The coefficients R_0 and T_0 are the plane-wave reflection and transmission coefficients for the unperturbed flat interface. The continuity equations which need to be satisfied at the water sediment interface are

$$\rho_w \phi_w = \rho_{se} \phi_{se} \tag{8}$$

and

$$-h'(x)\frac{\partial \phi_w}{\partial x} + \frac{\partial \phi_w}{\partial z} = -h'(x)\frac{\partial \phi_{se}}{\partial x} + \frac{\partial \phi_{se}}{\partial z}. \tag{9}$$

Substituting (6) and (7) into (8) and (9) and expanding for $h(x)$ and $h'(x)$ small, the leading order expression for $a(\lambda)$ and $b(\lambda)$ are obtained. We will not carry out the straightforward details here. It is important to note, however, that the coefficients $a(\lambda)$ for the backscattered direction (negative values of the wavenumber k_x) depend upon $\tilde{h}(|k_0|+|k_x|)$ whereas the coefficients for the scattered field in the forward direction depend upon $\tilde{h}(|k_0|-|k_x|)$, where $\tilde{h}$ denotes the Fourier Transform of h.

We now consider a particular set of rough interfaces. These interfaces have the form

$$h(x) = \epsilon e^{-x^2/(2\sigma^2)} cos(k_0 x). \tag{10}$$

The parameter k_0 allows us to control the wavelength of the perturbation and σ its effective lateral extent. The amplitude of the perturbation is controlled by ϵ. The Fourier Transform of the surface as defined in (10) is

$$\tilde{h}(k) = \frac{\epsilon\sigma}{4\sqrt{\pi/2}}(e^{-\sigma^2(k-k_0)^2/2} + e^{-\sigma^2(k+k_0)^2/2}). \tag{11}$$

In the numerical computations the amplitude ϵ will be decreased linearly as a function of frequency, in order that the height of the perturbation remain a fixed ratio of a wavelength.

We can make a simple prediction of the frequency dependence of these spectral curves. Recall that the amplitude of the forward scattered field is approximately proportional to $\tilde{h}(k - k_{in})$ or

$$T(k) \propto e^{-\sigma^2(k-k_{in}-k_0)^2/2} + e^{-\sigma^2(k-k_{in}+k_0)^2/2}. \tag{12}$$

We also recall that for $k > k_c = 2\pi f/c_{se}$ the energy in the bottom is evanescent. We first consider the situation where the acoustic wavelength is smaller than the wavelength of the interface roughness. Considering the second exponential in (12) and writing $k = k_c q$, $k_{in} = 2\pi f \cos(\theta_g)/c_w$ and $k_0 = \alpha\pi$, where θ_g denotes grazing angle, we derive the relation

$$q = \frac{c_{se}}{c_w}\cos(\theta_g) - \frac{\alpha c_{se}}{2f} \tag{13}$$

in order that the exponential's argument be zero. The maximum possible of q is unity before the dominantly scattered energy in the bottom is evanescent (recall that $k = k_c q$) and the value of the frequency for which this occurs is given by

$$f_{max} = \frac{\alpha c_{se}}{2[c_{se}/c_w \cos(\theta_g) - 1]}. \tag{14}$$

We do not expect significant energy to propagate in the bottom for acoustic frequencies much greater than this value.

On the other hand, if k_0 is very large then there will not be significant scattering in the bottom for frequencies which are too small. Following a similar analysis as before, it can be estimated that there will only be significant enhanced propagation in the sediment for

$$\frac{\alpha c_{se}}{2[c_{se}/c_w \cos(\theta_g) + 1]} \leq f \leq \frac{\alpha c_{se}}{2[c_{se}/c_w \cos(\theta_g) - 1]}. \tag{15}$$

For small values of frequency, the evanescent energy which is present in the sediment, regardless of the interface roughness, may dominate.

Another feature which can be derived from (12) is that for a frequency lying in the bounds of (15), the direction of the dominant energy in the sediment is in the $-k_x$ direction for the lower value of the frequency, increases to normal incidence with increasing frequency and then finally at the maximum frequency is nearly horizontal in the $+k_x$ direction.

3. NUMERICAL EXAMPLES

We consider an air-filled steel-shelled cylinder (c_p = 5950 m/s, c_{shear} = 3240 m/s and $\rho = 7.7g/cm^3$) of 15 mm thickness and outer radius 0.25 m. We consider an incident field with a plane-wave spectrum of the form

$$w(k_x) = exp(-(k_x - k_x^0)^2/{\sigma_b}^2) \tag{16}$$

where $k_x^0 = \omega \cos(20°)/c_w$ and $\sigma_b = 0.025\omega/c_w$ will be used in the computations. Thus a beam centred about the grazing angle of $\theta_g = 20°$ is produced, directed towards the centre of the cylinder. For angles approximately $\pm 3.85°$ on either side of 20°, the beam has e^{-1} of its maximum amplitude. In Fig. 2 we show the spectrum of the backscattered field at a receiver located at x=-2.747 m and z=1 m relative to the cylinder centre when the surrounding fluid has parameters c_p = 1700 m/s and ρ = 1500 kg/m^3. This receiver location corresponds to a direction of $-20°$ with respect to the cylinder centre (measured from the horizontal axis); thus we are considering a monostatic scattering geometry. We have computed the scattered field in two ways: (1) we used the plane-wave decomposition method (solid line) (2) we solved the scattering problem explicitly in terms of the Fourier-Bessel series for different incident plane-wave directions and then summed the results to produce the beam response (dashed line). As can be seen the two methods give essentially identical results

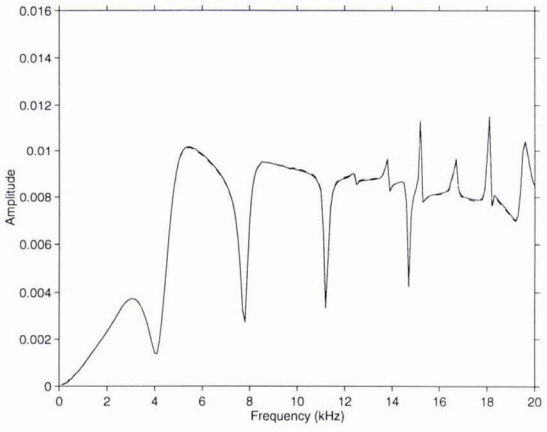

Figure 2: *Spectrum of backscattered field for surrounding fluid* $c_p = 1700m/s, \rho = 1500kg/m^3$ *as computed for an incident beam, using the plane-wave decomposition method(solid line) and a Fourier-Bessel series approach(dashed line)*

We now consider the incident beam to be in the water column ($c_p = 1500m/s, \rho = 1000kg/m^3$) and the cylinder in the sediment ($c_p = 1700m/s$, $\rho = 1500kg/m^3$) buried 0.5 m (2 radii) below the interface. For this sediment the critical grazing angle in the water column is equal to 28.1° and therefore the centre angle of the incident beam is 8° below critical. In Fig. 3a we show the field that is transmitted into the sediment for a frequency of 20 kHz. As can be seen, very little energy is transmitted into the sediment in this case. The fields that are scattered (the incident field is not shown) by a cylinder buried in the same sediment, but for a rough interface ($k_0 = 4\pi$), are shown in Figs. 3b and 3c for frequencies of 10 kHz and 20 kHz are shown. As can be seen, there is now significantly more energy in the bottom than in Fig. 3a. The scattered field is in fact strongest behind the cylinder where the total field would be a shadow zone. It can also be observed that directionality of the field is different for the two frequencies. This is in accordance with the predictions from (12). It can also be seen that the most energy is, in fact, backscattered at angles close to 90° back into the water column and that the amount of energy which reaches the receiver position is relatively small. In these and following computations, the value of ϵ is varied with frequency so as to be $\lambda/20$ ($\lambda \equiv$ wavelength) and σ in (10) is equal to 2. The roughness patch has its largest amplitude directly above the cylinder centre.

In Fig. 4 we show a plot of the backscattered spectral amplitudes for various rough interfaces. It can be seen that the Gaussian and flat bathymetries produce almost the same spectral response. The sinusoidal bathymetry with $k_0 = 4\pi$ produces a spectral curve which is significantly higher than the no-roughness curve for $f \geq 8kHz$. The spectral curve for the sinusoidal bathymetry with $k_0 = 0.75\pi$ is initially higher than the no-roughness curve but approaches it for increasing frequency, which is consistent with the behaviour as predicted by (15). The level of backscatter for the $k_0 = 4\pi$ curve is approximately equal to 2% of the level for the freespace curve of Fig. 2.

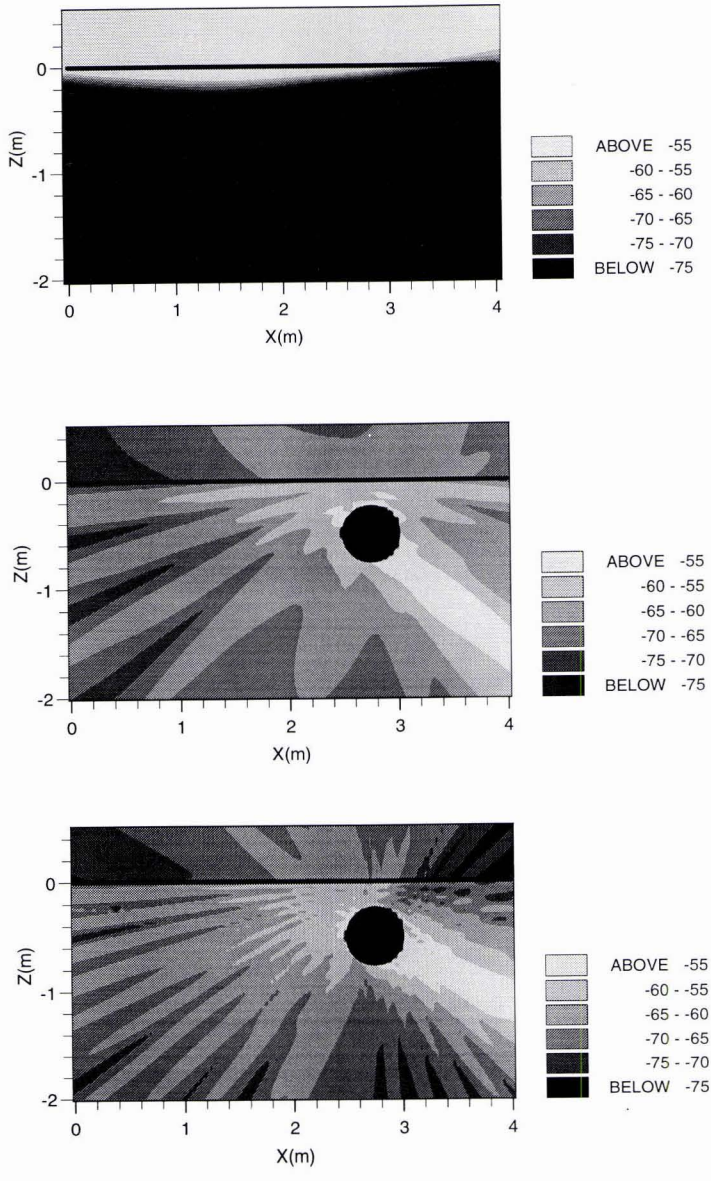

Figure 3: *Top figure is incident pressure field at 20 kHz; second figure is the pressure field scattered by the cylinder at 10 kHz for a rough interface ($k_0 = 4\pi$); third figure is the scattered pressure field at 20 kHz for the rough interface*

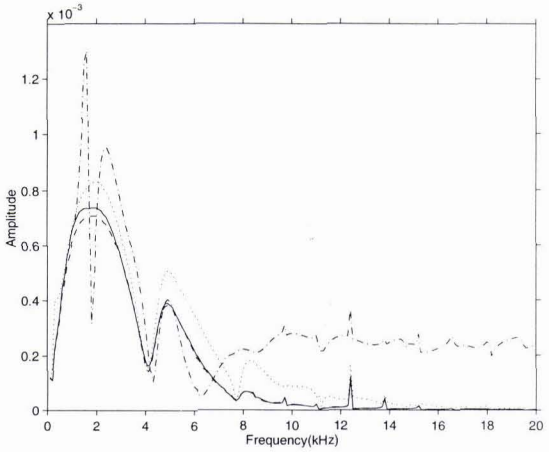

Figure 4: *Backscattered energy spectra for different types of surface roughnesses: no roughness (solid line), Gaussian profile (dashed), sinusoidal ($k_0 = 4\pi$) (dash-dotted) and sinusoidal ($k_0 = 0.75\pi$) (dotted)*

We now consider a flat interface and an interface with $k_0 = 4\pi$, in the case that the sediment has an attenuation of $0.5dB/\lambda$. The spectral curves for this case are shown in Fig. 5. As would be expected, the levels are less in this case and decrease with frequency. Also, note that most of the resonance structure of the curves has disappeared.

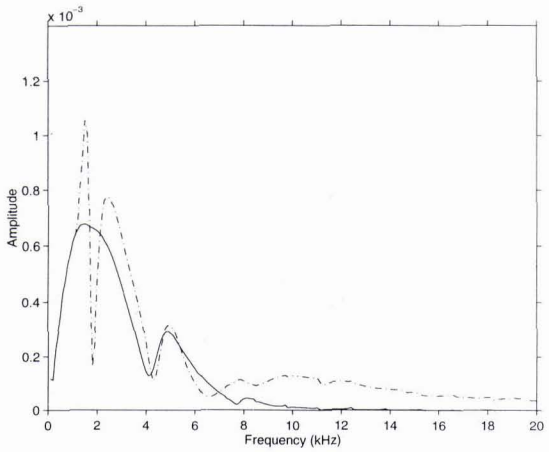

Figure 5: *Backscattered energy spectra for no roughness (solid line) and sinusoidal ($k_0 = 4\pi$) (dash-dotted) interfaces in the case that there is an attenuation of 0.5 dB/λ in the sediment*

We have seen that the presence of a rough interface increases the amount of energy in the sediment and leads to an increased amount of backscatter from the cylinder. However, there will also be increased backscatter from the interface itself and this will interfere with the backscattered energy from the cylinder. In Fig. 6 below we show the computed backscattered energy from the interface (ignoring the flat interface specular component) as a function of frequency (solid line) as well as the backscattered energy from the cylinder. As can be seen the energy backscattered from the interface dominates until f=10 kHz. Of course, in the time domain it maybe possible to separate the two types of energy, even when the reverberant energy dominates, by using appropriate filtering techniques.

Finally, we consider the modelling issue of when a single scatter approximation may be used. That is, instead of computing all the multiple interactions between the cylinder and the water/sediment interface above it, we may

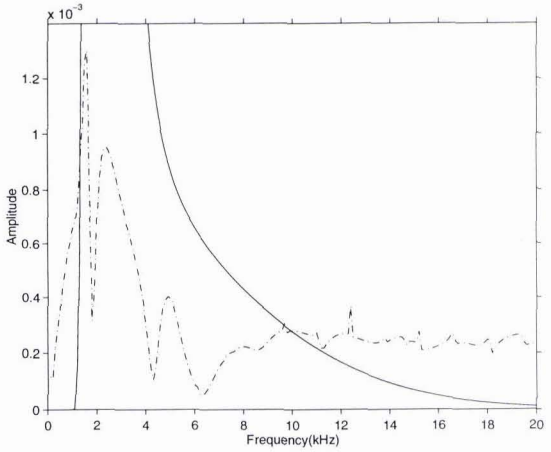

Figure 6: *Backscattered field from the interface (solid line), and backscattered signal from buried cylinder (dash-dotted) for sinusoidal ($k_0 = 4\pi$) interface*

approximate the scattering process as an incident field upon the cylinder, accounting for transmission through the rough interface, a single, free-space scattering (using the parameters of the surrounding sediment), and then transmission back into the water column. For the retransmission back into the water column from the sediment we consider two subcases; (1) we use the transmission coefficient for the flat interface (2) we account for the roughness for this second transmission process. There are computational advantages if the single scatter approximation is accurate; a variety of propagation codes can be used to propagate the incident field up to the scatterer and to propagate the scattered field away from the object. The scattering from the object can be computed using a free-space code. This type of approach has been used previously by other authors for waveguide scattering problems (see, for example, [9],[10]). In Fig. 7 we show the backscattered spectral curves using the exact solution (solid line), using the single scatter approximation with the flat interface transmission coefficients for transmission back into the water (dashed line), and the single scatter approximation with the rough interface transmission coefficients for transmission back into the water. As can be seen all three curves are very close, except near the strong peaks at

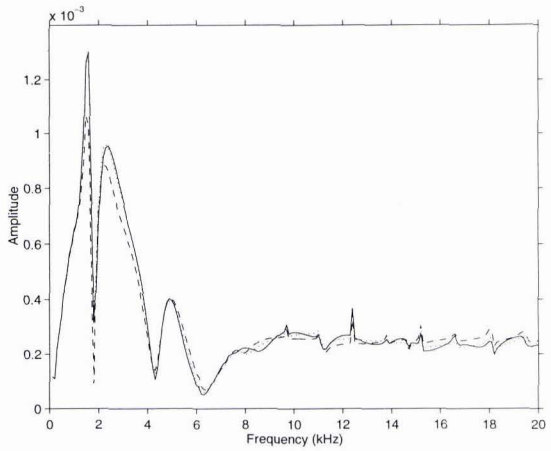

Figure 7: *Backscattered field from the cylinder for the rough interface ($k_0 = 4\pi$) using the exact solution (solid line), the single scatter approximation with simple retransmission back into water (dashed line), and the single scatter approximation with rough interface retransmission back into the water (dotted line).*

approximately 2kHz where using the correct rough interface transmission coefficients for retransmission into the water has a noticeable effect.

4. SUMMARY

It has been showed that the plane-wave decomposition method can be combined in a straightforward fashion with perturbation theory to compute scattering from objects buried below a rough interface. It was found that, for the case where the energy would normally be evanescent in the bottom, a rough interface can significantly increase the amount of object backscattered energy observed at a receiver in the water column. In fact, at sufficiently high frequencies this energy is higher than the energy backscattered from the interface itself (ignoring the specular component from the flat interface). The amount of energy and the directionality of the energy in the bottom depends upon the wavelength of the interface roughness. Finally, we have shown that a simpler (and computationally faster) single-scatter approximation can probably be used in many computations.

References

[1] J.L. Lopes, "Observations of anomalous acoustic penetration into sediment at shallow grazing angles", J. Acoust. Soc. Am., **99**, p. 2473, 1996.

[2] N.P. Chotiros, "Acoustic penetration of ocean sediments in the context of Biot's theory", J. Acoust. Soc. Am., **99**, p. 2474, 1996.

[3] N.P. Chotiros, "Biot model of sound propagation in water-saturated sand", J. Acoust. Soc. Am., **97**, pp.199–214, 1995.

[4] D.R. Jackson, J.E. Moe, E.I. Thorsos, and K.L. Williams, "Subcritical penetration of sandy sediments due to interface roughness", J. Acoust. Soc. Am., **99**, p.2474, 1996.

[5] B.L.N. Kennett, "Reflection operator methods for elastic waves I–Irregular interfaces and regions", Wave Motion, **6**, pp.407–418, 1984.

[6] J.A. Fawcett, "A plane-wave decomposition method for modeling scattering from objects and bathymetry in a waveguide", J. Acoust. Soc. Am., **100**, pp.183–192, 1996.

[7] E.I. Thorsos, "The accuracy of perturbation theory for acoustic penetration of sediment due to interface roughness", J. Acoust. Soc. Am., **99**, p.2475, 1996.

[8] G.C. Bishop and J. Smith, "Scattering from an elastic shell and a rough fluid-elastic interface: Theory", J. Acoust. Soc. Am., **101**, pp.767–788, 1997.

[9] F. Ingenito, "Scattering from an object in a stratified medium", J. Acoust. Soc. Am., **82**, pp.2051–2059, 1987.

[10] M.D. Collins and M.F. Werby, "A parabolic equation model for scattering in the ocean", J. Acoust. Soc. Am., **85**, pp.1895–1902, 1989.